Electronic Supplementary Material (ESI) for Journal of Materials Chemistry C.

Second harmonic generation in nonlinear optical crystal formed of propellane-type molecule

A. Miniewicz[1*], S. Bartkiewicz[1], E. Wojaczynska[1], T. Galica[1], R. Zalesny[1] and R. Jakubas[2]

[1]*Faculty of Chemistry of the Wroclaw University of Science and Technology, Wybrzeze Wyspianskiego 27, 50-373 Wroclaw, Poland*

[2]*Faculty of Chemistry, University of Wroclaw, Joliot-Curie 14, 50-383 Wroclaw, Poland*

*e-mail: Andrzej.miniewicz@pwr.edu.pl

Synthesis and characterization of DDDDP

DDDDP ($C_{18}H_{17}N_4O_6$) compound (16,20-dinitro-(3,4,8,9)-dibenzo-2,7-dioxa-5,10-diaza[4.4.4]propellane) has been synthesized according to following procedure: a mixture of 1.2-cyclohexanedione (1.00 g, 8.9 mmol) and 2-amino-5-nitrophenol (2.74 g, 17.8 mmol, 2 eq.) was dissolved in 30 mL of ethanol and heated under reflux for 8 h. The formed solid was filtered off and next purified by a column chromatography on silica. Unreacted starting materials were eluted with n-hexane-ethyl acetate mixture (1:1 v/v). Then elution with acetone yielded the desired compound as a yellow fraction. Recrystallization from ethanol resulted in yellow solid powder, yielding 1.09 g (32%) of product. Elemental analysis for $C_{18}H_{17}N_4O_6$ (384.35): Calcd. C, 56.25; H, 4.196; N, 14.58. Found: C, 55.94; H, 4.245; N, 14.16 shows good agreement. DDDDP melts and decomposes in the range of 271–282 ^{o}C. ^{1}H NMR data measured for DDDDP in DMSO-d_6, δ, ppm: 8.48 (s, 2H, NH), 7.70 (dd, J_1 = 8.8 Hz, J_2 = 2.5 Hz, 2H, H_{17},H_{21}), 7.44 (d, J = 2.5 Hz, 2H, H_{15},H_{19}), 6.79 (d, J = 8.8 Hz, 2H, H_{18},H_{22}), 1.86 (d, J = 13.0 Hz, 2H, Cy), 1.50-1.64 (m, 6H, Cy) are in good agreement with the literature ones [25], the presence of NO_2 groups results with some de-shielding of protons with respect to the non-NO_2 substituted compound. In ^{13}C NMR spectrum collected in DMSO-d_6 (δ, ppm: 140.1, 139.3, 137.5, 119.2 (CH), 113.7 (CH), 112.1 (CH), 82.3, 32.6 (CH_2), 22.8 (CH_2)) six signals in the aromatic region (110-160 ppm) are accompanied by three cyclohexyl peaks, with C_1/C_6 signal shifted to 82.6 ppm. High Resolution Mass Spectrometry (ESI-TOF): calculated for $C_{18}H_{17}N_4O_6^-$ ([M-H]$^-$) 383.0992; found 383.0991. The infrared spectra of DDDDP measured in KBr pellet show characteristic bands: 3316 (ν(NH)), 2946, 1885, 1600, 1516, 1275, 1225, 1078, 1013 cm^{-1}.

Below, in Figure S1 we show ^{1}H NMR data measured for DDDDP in DMSO-d_6 and in Figure S2 ^{13}C NMR spectrum collected in DMSO-d_6.

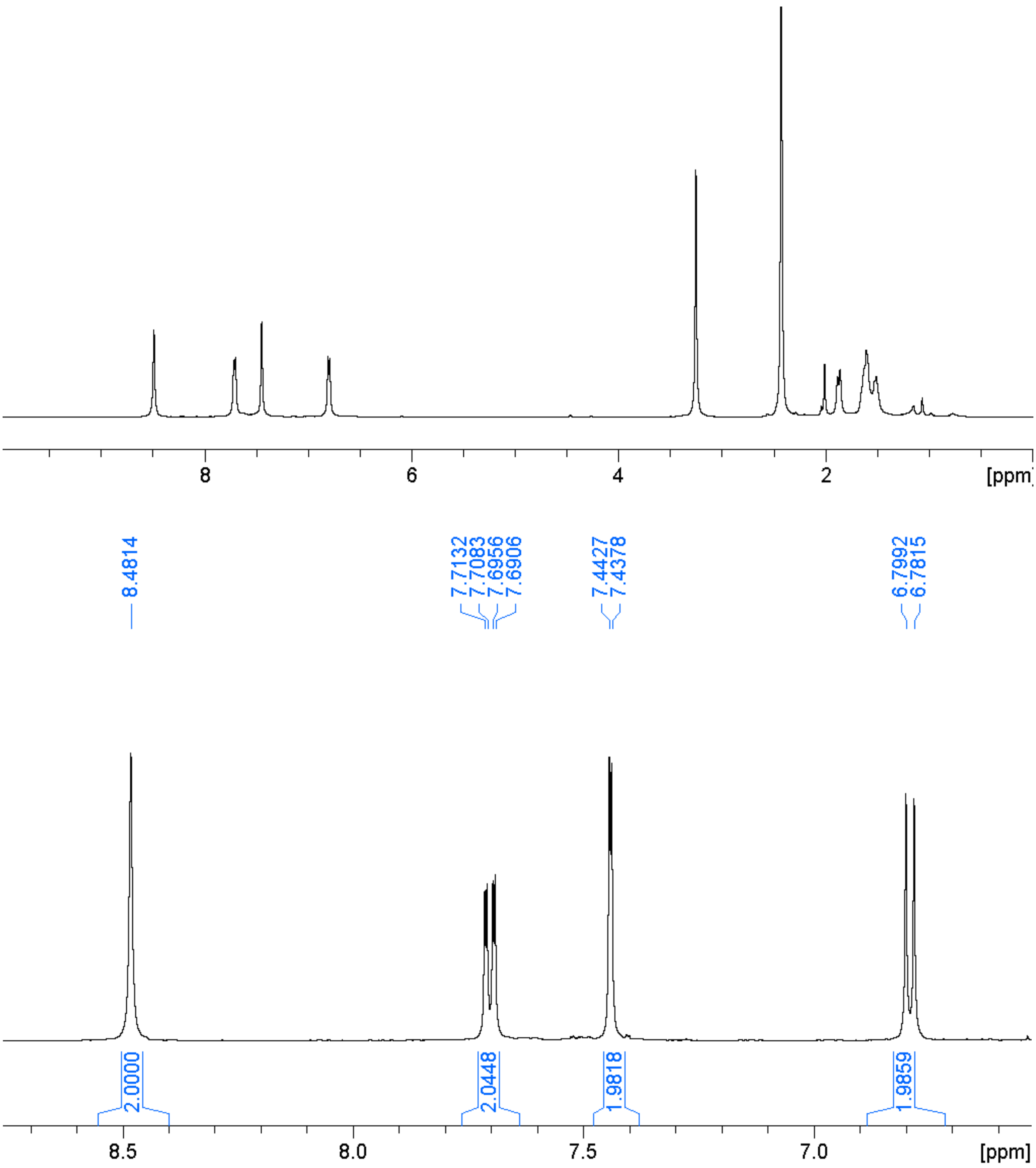
8
6
4
2
[ppm]
8.4814
7.7132
7.7083
7.6956
7.6906
7.4427
7.4378
6.7992
6.7815
2.0000
2.0448
1.9818
1.9859
8.5
8.0
7.5
7.0
[ppm]

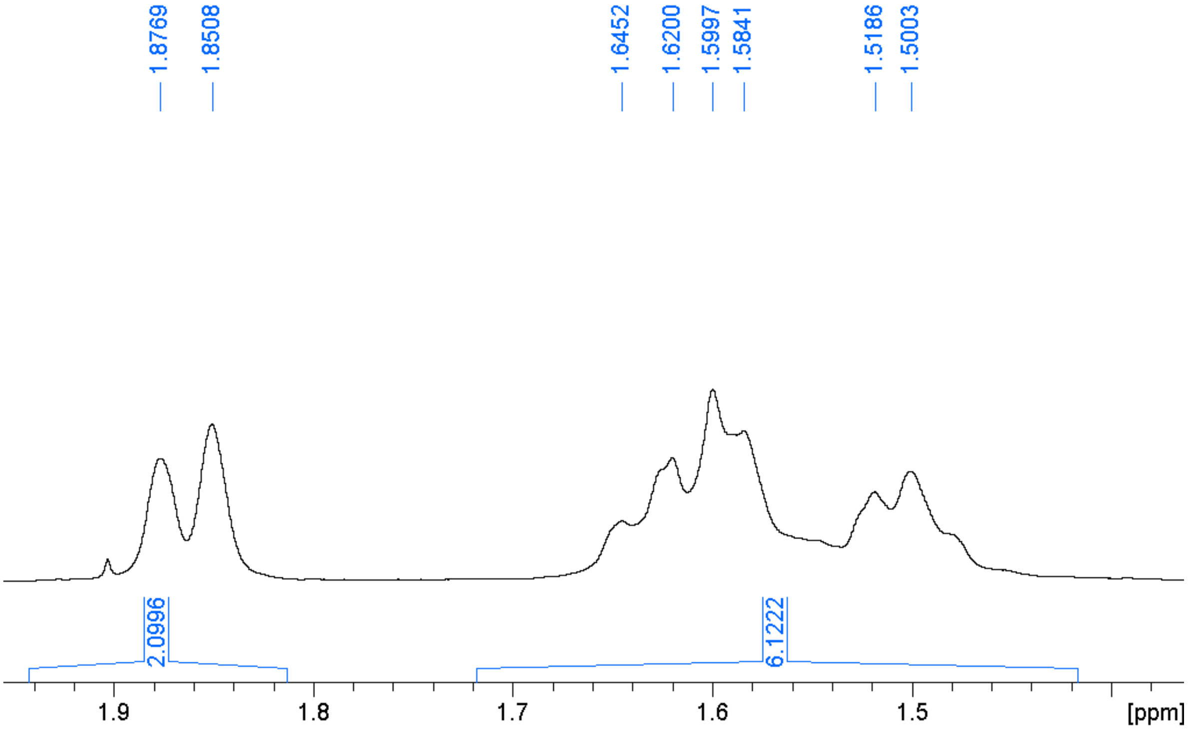

Figure S1. ${}^{1}H$ NMR spectrum of DDDDP (500 MHz, DMSO-d_6, 300 K) and its fragments

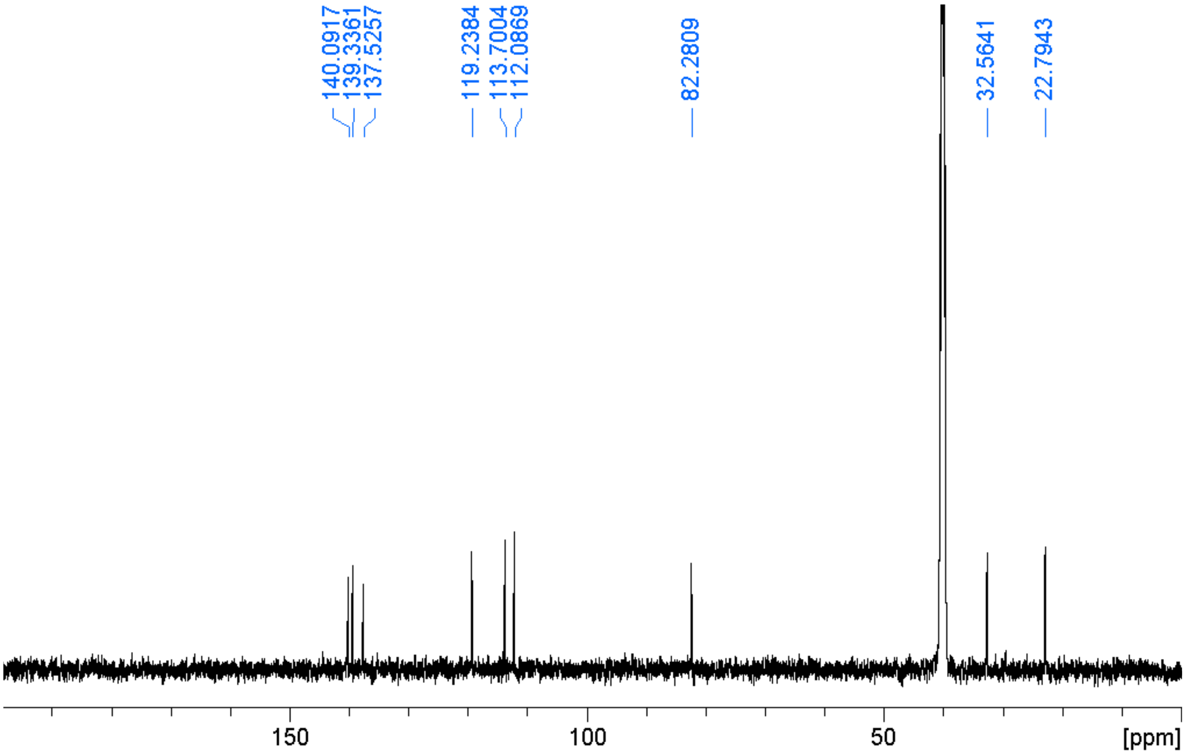

Figure S2. ${}^{13}C$ NMR spectrum of DDDDP (125 MHz, DMSO-d_6, 300 K)

Crystal structure

The crystals of 16,20-dinitro-(3,4,8,9)-dibenzo-2,7-dioxa-5,10-diaza[4.4.4]propellane were crystalized from methanol solution by slow evaporation method at room temperature. X-ray data collection was carried out by means of a 4-circle diffractometer equipped with a CCD detector. Data collection and reduction were done with CrysAlisPro software [1]. The X-ray experiment was conducted in conditions of darkness. The structure was solved with SHELXS and refined with SHELXL software [2,3]. All non-hydrogen atoms were refined anisotropically. All hydrogens were found in a Fourier difference map and refined with $U_{iso}(H) = 1.2\ U_{eq}(C)$. The studied crystal was twinned, nevertheless it was possible to determine its structure. The proportions of twin components were 59% and 41%. The visualization of the structure taken at 294 K was prepared with the Mercury CSD 3.3 program [4]. Molecular packing projections along three crystallographic axes are shown in Fig. S3.

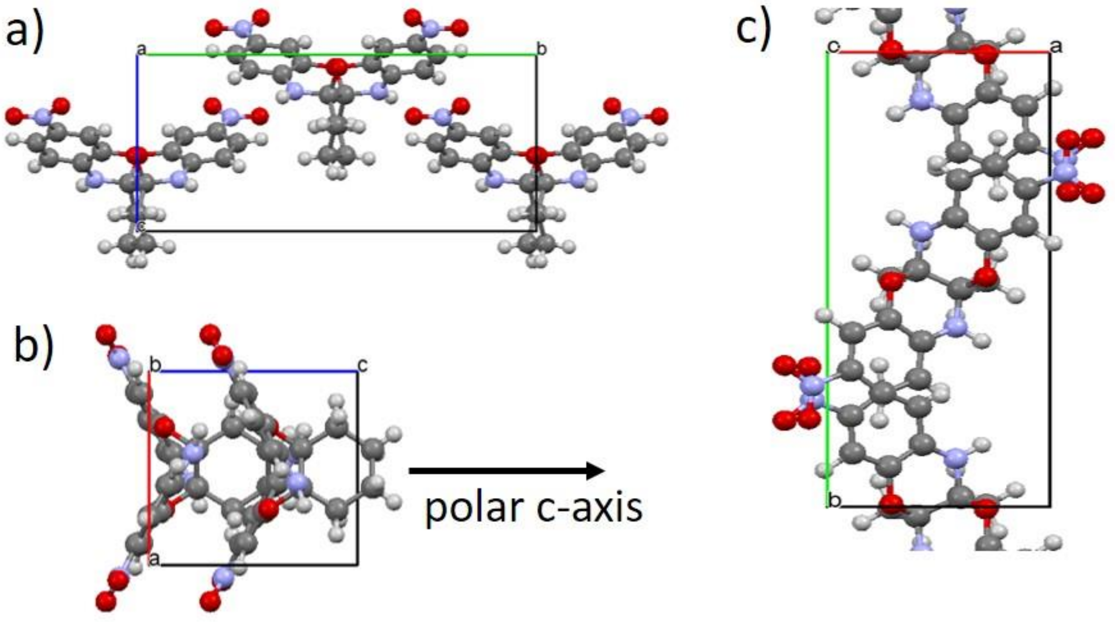

Figure S3. Molecular packing projection along the three orthogonal DDDDP crystal axes: ***a*** a); ***b*** b) and ***c*** c).

Measured and calculated powder X-ray diffraction spectra are shown in Fig. S4.

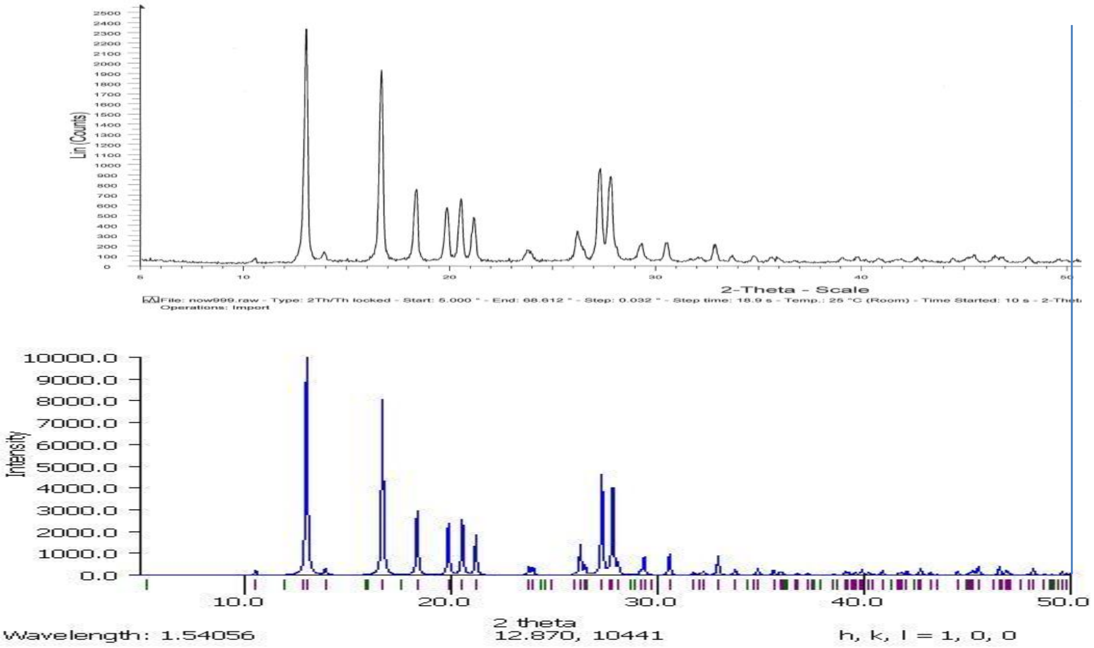

Figure S4. Comparison of measured (a) and calculated (b) PXRD spectra of DDDDP compound.

Calculations of polarizability and first hyperpolarizability

Table S1. The comparison of static (i.e. frequency-independent) molecular (hyper)polarizabilities computed using density functional theory and *ab initio* MP2 method. All values are given in au and were obtained with 6-31+G* basis set.

	α_{xx}	α_{yy}	α_{zz}	$<\alpha>$	β_{zxx}	β_{zzz}
MP2	275.81	303.26	194.48	257.85	-1222	-259
CAM-B3LYP	276.69	299.42	193.70	256.60	-1132	-221

The *ab initio* MP2 method is used here as reference to assess the accuracy of density functional theory. The results in Table 1 clearly demonstrate that the polarizability value predicted by CAM-B3LYP functional is in excellent agreement with the reference value and it holds both for diagonal components as well as for the trace of polarizability tensor ($<\alpha>$). Likewise, in the case of static first hyperpolarizability the agreement is very satisfactory and, for the component largest in terms of magnitude β_{zxx}, the relative error with respect to MP2 value is only 7.3%. To sum up, the property values reported in the manuscript obtained using density functional theory are quite accurately predicted, as demonstrated above by the comparison against *ab initio* MP2 results. The reported discrepancy between theory-based and experimental susceptibilities is thus largely due to approximations adopted in the physical model.

Note about units:

To the Table 2: The polarizability α_{ij} calculated by quantum chemical methods is given in atomic units (a.u.). Atomic unit of polarizability has the dimension of volume, and its numerical values are expressed in units of $(a_0)^3$, where $a_0 \approx 0.052918$ nm is the Bohr radius. In SI units 1 a.u. = 1.648773x10^{-41} C·m^2/V, basing on conversion via $4\pi\varepsilon_0 a_0^3$, with $\varepsilon_0 \approx 8.854 \times 10^{-12}$ (F/m).

To the Table 3: The molecular first hyperpolarizabilities [38] are expressed in Table 3 in atomic units or of (dipole moment)^3/energy^2:

$$\beta = \frac{e^3 a_0^3}{E_h^2} = \frac{a_0^5}{e} \tag{3}$$

where e is the electron charge and $E_h = \frac{e^2}{a_0}$ is the ionization energy of hydrogen (a Hartree). Therefore in electrostatic units (esu) first hyperpolarizability is given as cm^{5}statcoulomb^{-1} which is identical to cm^{5}esu^{-1}. These units are simply referred to as esu in Table 3. The conversion factor between atomic units and esu is as follows: 1 atomic unit =8.641 x 10^{-33} cm^{5}esu^{-1}, while in SI units 1 a.u. =3.206 x 10^{-53} C^{3}m^{3}J^{-2}.

To the Table 4: In the literature instead of NLO susceptibilities $\chi_{ijk}^{(2)}$ usually nonlinear optical coefficients $d_{ijk}^{(2)}$ are given. In the case of SHG process $d_{ijk}^{(2)}(-2\omega;\omega,\omega) = {}^1\!/_2\,\chi_{ijk}^{(2)}(-2\omega;\omega,\omega)$. These coefficients in handbooks of NLO optics are presented in contracted matrix notation as d_{il} (where i=1, 2, 3 and l= 1,…6) and given in units of pm/V.

Measurements of powder SHG efficiency of DDDDP

We assembled the standard experimental setup for powder SGH measurement using a SURELITE II Nd:YAG pulsed laser as a pumping source with removed SHG and THG units for obtaining spectrally pure infrared beam. The laser pulse duration $\tau = 10$ ns, wavelength $\lambda = 1064$ nm, tunable pulse energy from 20 mJ up to 500 mJ, pulse repetition rate 10 Hz, unfocused light beam with diameter of ~ 7 mm. Detection of doubled in frequency radiation at 532 nm wavelength has been done with an optical fiber Ocean Optics USB 2000 spectrometer equipped with a diode array detector coupled to the computer. Integration time was set at 380 ms allowing for averaging over 3 pulses. For more accurate SH line-width measurements the Avantes AvaSpec-ULS2048 fiber-optic spectrometer was used (cf. Figure S5). The fiber entrance aperture collects only a small portion of the SHG signal scattered in a wide angle from the sample, therefore the reference powder is necessary to evaluate a new material performance. Powders of the investigated compound as well as the powders of the reference compounds (KDP, urea) were contained between two microscope glass plates. SHG light was collected using a multimode optical fiber in backscattering geometry. The laser pulse energy was controlled with the time delay of Pockels cell opening with respect to the flash lamp pulse and precisely measured with the laser energy meter. The Pockels cell was placed in the laser cavity. Taking the square root of intensity of SHG signal measured by spectrometer with CCD detector dynamic range of 4096, we were able to calculate the SHG conversion efficiency factor for DDDDP material. The main source of error comes from the difference in grain sizes as well as, to a minor extent, to refractive indices of the studied material.

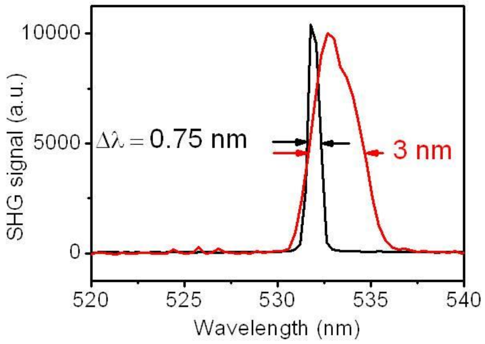

Figure S5. SHG (532 nm) signal linewidths for DDDDP measured with Ocean Optics USB 2000 (red curve, FWHM = 3 nm) and Avantes (black curve, FWHM = 0.75 nm) fiber-optic spectrometers, respectively.

The powder of DDDDP compound is yellowish in color. In Fig. S6 we show absorption spectrum of DDDP dissolved in two solvents: DMSO and methanol. Solubility of DDDDP is considerably higher in DMSO than in methanol. The absorption edge starts around 450 nm and maxima of absorption are 338 nm and 373 nm in DMSO and methanol, respectively. The spectra of DDDDP show that the SHG signal at 532 nm is far from resonance and the material is transparent at least in the range of 460 nm to 700 nm.

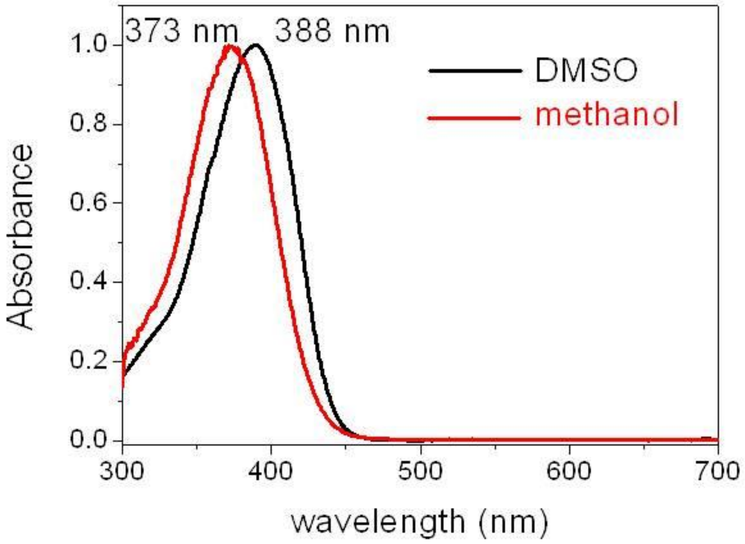

Figure S6. Normalized spectra of DDDDP compound in two polar solvents: DMSO and methanol.

References

[1] CrysAlisPro Software System, version 1.171.38.41, (2016), Rigaku Corporation, Oxford, U.K.

[2] Sheldrick, G. M. A short history of SHELX. *Acta Crystallogr. A: Found. Crystallogr.*, **2008**, *64*, 112−122.

[3] Sheldrick, G. M. Crystal structure refinement with SHELXL. *Acta Crystallogr. C: Struct. Chem.* **2015**, *71*, 3−8.

[4] Macrae, C. F.; Edgington, P. R.; McCabe, P.; Pidcock, E.; Shields, G. P.; Taylor, R.; Towler, M.; van de Streek, J. Mercury: Visualization and Analysis of Crystal Structures. *J. Appl. Crystallogr.* **2006**, *39*, 453–457.